Identification of Combustion Intermediates in Low-Pressure Premixed Pyridine/Oxygen/Argon Flames

ARTICLE *in* THE JOURNAL OF PHYSICAL CHEMISTRY A · DECEMBER 2008

Impact Factor: 2.69 · DOI: 10.1021/jp8066537 · Source: PubMed

5 AUTHORS, INCLUDING:

Zhen-Yu Tian
Chinese Academy of Sciences
66 PUBLICATIONS **890** CITATIONS
SEE PROFILE

Taichang Zhang
Chinese Academy of Sciences
32 PUBLICATIONS **398** CITATIONS
SEE PROFILE

THE JOURNAL OF PHYSICAL CHEMISTRY A

Article

Identification of Combustion Intermediates in Low-Pressure Premixed Pyridine/Oxygen/Argon Flames

Zhenyu Tian, Yuyang Li, Taichang Zhang, Aiguo Zhu, and Fei Qi

J. Phys. Chem. A, **2008**, 112 (51), 13549-13555 • DOI: 10.1021/jp8066537 • Publication Date (Web): 19 November 2008

Identification of Combustion Intermediates in Low-Pressure Premixed Pyridine/Oxygen/Argon Flames

Zhenyu Tian, Yuyang Li, Taichang Zhang, Aiguo Zhu, and Fei Qi*

National Synchrotron Radiation Laboratory, University of Science and Technology of China, Hefei, Anhui 230029, People's Republic of China

Received: July 27, 2008; Revised Manuscript Received: September 13, 2008

Combustion intermediates of two low-pressure premixed pyridine/oxygen flames with respective equivalence ratios of 0.56 (C/O/N = 1:4.83:0.20) and 2.10 (C/O/N = 1:1.29:0.20) have been identified with tunable synchrotron vacuum ultraviolet (VUV) photoionization and molecular-beam mass spectrometry techniques. About 80 intermediates in the rich flame and 60 intermediates in the lean flame, including nitrogenous, oxygenated, and hydrocarbon intermediates, have been identified by measurements of photoionization mass spectra and photoionization efficiency spectra. Some radicals and new nitrogenous intermediates are identified in the present work. The experimental results are useful for studying the conversion of volatile nitrogen compounds and understanding the formation mechanism of NO_x in flames of nitrogenous fuels.

1. Introduction

The combustion chemistry of nitrogenous compounds is of great interest, which derives from the role of nitrogen oxides, collectively referred to NO_x, that has detrimental effects on the environment and human health. Increasingly stringent environmental regulations require more effective approaches for the control of NO_x formation from combustion. As the major species of nitrogen oxides, NO is known to be formed in three ways:[1] (1) oxidation of atmospheric nitrogen by the "thermal" mechanism to form NO in high-temperature circumstances, such as flames; (2) "prompt" NO in hydrocarbon flames is formed primarily by a reaction sequence that is initiated by the rapid reaction of hydrocarbon radicals with molecular nitrogen, leading to formation of amines or cyanic compounds that subsequently convert to NO; (3) "fuel" NO is formed at comparatively low temperatures from the nitrogenous compounds in the fuel. Combustion of coal and coal-derived fuels containing nitrogen in heterocyclic structures, e.g. pyridine and pyrrole ring systems, is considered to be the principal source of NO_x emissions.[1] It is also believed that the nitrogenous components in heavy oils have similar structures. Therefore, the flame chemistry of pyridine, the simplest six-membered nitrogenous heterocyclic aromatic, is significant for understanding the mechanism of nitrogen conversion in fuels.

There are some published papers related to pyrolysis and oxidation of pyridine. For pyrolysis studies, few products were detected and its thermal decomposition mechanism was proposed.[2−11] In 1886, Roth studied pyrolysis of pyridine by passing it through a hot glass tube, and observed hydrogen cyanide and bipyridine as the major products.[2] In 1962, thermal decomposition of pyridine was studied in a flow reactor by Hurd and Simon.[3] They reported acrylonitrile, acetonitrile, benzonitrile, and quinoline as the major nitrogenous products, and concluded that the primary step in pyrolysis of pyridine was the rupture of the ring. Axworthy et al.[4] extended Hurd's results and developed a detailed kinetic model. In 1980, Houser et al.[5] studied the kinetics of pyrolysis of pyridine at 1150−1320 K. They proposed that C−H bond is more likely to be broken than the C−C bond and pointed out that HCN is a secondary product rather than a direct product from pyridine pyrolysis.

Recently, shock tube studies of pyridine pyrolysis were performed over the temperature range of 1300−2400 K.[6−11] Kern et al.[6] confirmed Houser's assumption that pyrolysis of pyridine was initiated with a ring hydrogen fission. Leidreiber and Wagner[7] measured the rate of decomposition of pyridine at temperatures between 1700 and 2000 K. Mackie and co-workers[8] identified acetylene, cyanoacetylene, HCN, and H_2 as major end-products at high temperatures. Other products reported were C_4H_2, CH_4, C_6H_2, PhCN, H_2CCHCN, C_6H_6, CH_3CN, HCCCHCHCN, and C_3H_4. In 1997, Kiefer et al.[9] investigated thermal decomposition of pyridine in shock waves and proposed a free radical chain reaction with initiation by ring C−H fission. Later, Hore et al.[10] reported radical pathways in thermal decomposition of pyridine, indicating that *o*- and *m*-pyridyl radicals were sufficiently long-lived to initiate exchange reactions with hydrogen. More recently, Memon et al. used a shock tube and obtained the kinetics of pyridine decomposition in the temperature range of 1590−2335 K and with pressures between 2.2 and 3.4 atm.[11]

Compared with pyrolysis investigations of pyridine, few previous studies of its oxidation have been performed. Houser et al.[12] studied oxidation of pyridine in a flow reactor and reported the effect of pyridine/oxygen ratio on nitrogenous products. In 2000, Ikeda et al.[13] studied oxidation of pyridine in a single-pulse shock tube. They concluded that the oxidation was initiated both by unimolecular C−H bond fission and bimolecular reaction with O_2 to form *o*-pyridyl radical, which could further react with oxygenated species to give the pyridoxy radical. This radical mechanism was supported by Alzueta et al.,[14] who studied pyridine conversion in a quartz flow reactor in the temperature range of 700−1500 K.

As mentioned above, pyridine has been investigated as the precursor of NO_x extensively and most of these studies were focused on the end-product identification. However, end-product analysis cannot provide detailed mechanistic information of pyridine oxidation under combustion conditions. Experimental data related to combustion intermediates are scarce, especially

* Corresponding author. E-mail: fqi@ustc.edu.cn. Fax: +86-551-5141078. Phone: +86-551-3602125.

10.1021/jp8066537 CCC: $40.75
Published on Web 11/19/2008

for nitrogenous species and radicals which feature as key species in the formation of nitrogenous pollutants.

This paper presents the isomeric identification of intermediates and products in the pyridine flames, with the global objective of understanding of the combustion chemistry of nitrogenous compounds. In the present work, the lean and rich premixed pyridine flames are studied with the molecular-beam mass spectrometry (MBMS) and tunable synchrotron VUV photoionization techniques.[15−17] The high resolution of photoionization mass spectrometry (PIMS) and the tunable photon energy from synchrotron allow measurements of flame species and isomeric identification of intermediates by comparing photoionization efficiency (PIE) spectra with known PIE spectra or IEs of pure substances. About 80 intermediates in the rich flame and 60 intermediates in the lean flame are detected and identified. The comprehensive analysis of the observed species in the rich and lean pyridine flames involving the mole fraction profiles and kinetic modeling will be presented in the future.

2. Experimental Methods

The experiments were performed at the National Synchrotron Radiation Laboratory (NSRL), Hefei, China. The experimental setup has been reported elsewhere,[16,18,19] and only a brief description is given here. The apparatus is composed of a flame chamber, which contains a movable flat-flame burner (McKenna Burner) 6 cm in diameter, a differentially pumped chamber with a molecular-beam sampling system, and a photoionization chamber combined with a reflectron time-of-flight mass spectrometer (RTOF-MS). Flame species are sampled by a quartz cone-like nozzle with a 40° included angle and a ∼500 μm orifice at the tip. The sampled gas forms a molecular beam that then passes into a differentially pumped ionization region through a nickel skimmer. The molecular beam is crossed with the tunable synchrotron VUV light in the photoionization chamber and the photoions are collected and analyzed by RTOF-MS.[20] Then the ion signals are amplified by a preamplifier (VT120C, ORTEC) and recorded by a multiscaler (P7888, FAST Comtec) with a bin width of 2 ns. A digital delay generator (DG535, SRS) is used to trigger a pulsed power supply and the multiscaler as well.

A 1 m Seya-Namioka monochromator is used to disperse synchrotron radiation from a bending magnet beamline of the 800 MeV electron storage ring. The energy resolving power ($E/\Delta E$) is about 500 with the average photon flux of about 5×10^{10} photons/s. A lithium fluoride (LiF) window with 1.0 mm thickness is used to eliminate higher order harmonic radiation from the monochromator when the wavelength is longer than 105.0 nm. The photon flux is monitored by a silicon photodiode (SXUV-100, International Radiation Detectors, Inc.) to normalize ion signals.

Pyridine sample was purchased from Sinopharm Chemical Reagent Co., Ltd., Shanghai, China with a purity of pyridine ≥99.5%. No further purification was carried out for this work. The equivalence ratios of the two premixed flames are $\phi = 2.10$ (C/O/N = 1:1.29:0.20) and $\phi = 0.56$ (C/O/N = 1:4.83:0.20) at pressures of 4.00 kPa (30 Torr) and 2.66 kPa (20 Torr), respectively. Flow rates of O_2 and Ar are controlled by MKS mass flow controllers and flow rate of pyridine is controlled by a syringe pump (1000D, ISCO). The flow rates for pyridine, O_2, and Ar are 0.895 mL/min (liquid at room temperature), 0.800 standard liter per minute (SLM), and 0.900 SLM for the rich flame and 0.539 mL/min, 1.810 SLM, and 1.400 SLM for the lean flame. The cold gas velocities are 29.12 and 75.30 cm/s for the rich and lean flames, respectively. The equivalence ratio is calculated according to reaction 1.

$$C_5H_5N + 5.75O_2 \rightarrow 5CO_2 + NO + 2.5H_2O \qquad (1)$$

Here NO is considered as the final NO_x product since it is more stable than NO_2 at high temperatures.[14] The temperature is measured by using a 0.076-mm-diameter Pt/Pt−13%Rh thermocouple coated with a Y_2O_3−BeO anticatalytic ceramic to reduce catalytic effects. Maximum temperatures are measured to be 1750 and 1850 K for the rich and lean pyridine flames, respectively, with an estimated error of 100 K.

A series of mass spectra are measured with the variation of photon energy at the fixed burner position. The ion intensity, which is obtained by integration of the peak over the entire mass peak and subtraction of the baseline contribution for a specified mass, is normalized by the photon flux, and then plotted as a function of the photon energy, which yields PIE spectrum containing the information of ionization energies (IEs) of specific species. The ionization energies obtained from PIE measurements are helpful for identification of isomers or species with the same masses. Considering the cooling effect of molecular beam, the experimental error for determining IE in this study is ±0.05 eV for stable species and ±0.1 eV for some radicals because of the weak signal-to-noise ratio in these species.

3. Results and Discussion

A number of stable intermediates and unstable radicals are formed in the pyridine flames. Figure 1 shows photoionization mass spectra of the pyridine flames at the photon energy of 11.81 eV, taken at the sampling positions of 4.0 mm for the lean flame and 7.5 mm for the rich flame. Because these sampling positions are luminescent regions of the investigated flames in this work, and most of the flame species have strong signals and high signal-to-noise ratio at the chosen positions, partial ion signals are amplified with factors of 10−30 for different mass regions. As presented in Figure 1, a series of

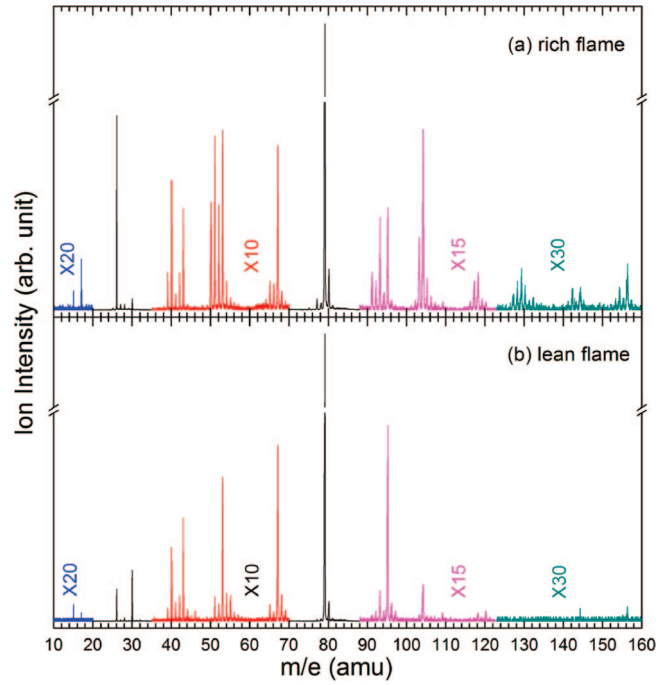

Figure 1. Photoionization mass spectra of the rich and the lean pyridine flames at the photon energy of 11.81 eV, taken at the sampling positions of 7.5 and 4.0 mm from the burner surface, respectively. Partial peaks are amplified with factors of 10−30 for different mass regions as shown in the figure.

TABLE 1: Combustion Intermediates Measured with Their Respective IE Values in the Fuel-Rich and -Lean Pyridine Flames

			IEs (eV)						IEs (eV)		
				this work[b]						this work[b]	
m/e	formula	species	lit.[a]	rich	lean	*m/e*	formula	species	lit.[a]	rich	lean
15	CH_3	methyl radical	9.84	9.82	9.82	79	C_5H_5N	pyridine	9.26	9.26	9.26
17	NH_3	ammonia	10.2	10.23	10.20	80	C_6H_8	1,3-cyclohexadiene	8.25	8.27	8.30
26	C_2H_2	acetylene	11.40	11.36	11.39	81	C_5H_7N	2-methylpyrrole	7.78	7.81	7.80
28	C_2H_4	ethylene	10.52	10.49	10.51	90	C_7H_6	5-ethenylidene−1,3-cyclopentadiene	8.29	8.28	
29	CH_3N	methanimine	9.97	9.98	10.00	91	C_6H_5N	phenylnitrene	8.0	8.13	8.07
30	NO	nitric oxide	9.26	9.26	9.26	92	C_7H_8	toluene	8.85	8.87	8.88
30	CH_2O	formaldehyde	10.88	10.88	10.89	93	C_6H_7N	aniline	7.72	7.78	
32	CH_3OH	methanol	10.84		10.87	93	C_6H_7N	picoline	9.04	9.02	9.03
39	C_3H_3	propargyl radical	8.67	8.68	8.68	94	C_6H_6O	phenol	8.49	8.51	8.53
40	*a*-C_3H_4	allene	9.83	9.81	9.81	95	C_5H_5NO	pyridine oxide	8.46	8.46	8.47
40	*p*-C_3H_4	propyne	10.36	10.33	10.36	95	C_5H_5NO	2-pyridinol	8.94	8.94	8.94
41	C_3H_5	allyl radical	8.18	8.18	8.21	96	C_7H_{12}	1-methylcyclohex-1-ene	8.67	8.66	8.68
41	C_2H_3N	methyl isonitrile	11.24	11.23	11.29	97	$C_6H_{11}N$	diallylamine	8.2		8.29
42	C_2H_2O	ketene	9.62	9.61	9.61	102	C_8H_6	phenylacetylene	8.82	8.85	
43	HCNO	fulminic acid	10.83	10.84	10.80	103	C_7H_5N	benzoisonitrile	9.19[d]	9.18	9.21
43	HNCO	isocyanic acid	11.60	11.55	11.58	103	C_7H_5N	benzonitrile	9.71	9.70	
44	C_2H_4O	ethenol	9.33	9.35	9.37	104	$C_6H_4N_2$	3-pyridinecarbonitrile	10.10	9.96	10.03
44	C_2H_4O	acetaldehyde	10.23	10.24	10.22	105	C_8H_9	4-methylbenzyl radical	7.46	7.50	
45	CH_3NO	formamide	10.5		10.49	105	C_7H_7N	*N*-phenylmethanimine	8.73	8.83	
46	CH_2O_2	formic acid	11.33		11.33	105	C_7H_7N	2-vinylpyridine	8.92		8.98
50	C_4H_2	1,3-butadiyne	10.17	10.18	10.19	106	C_8H_{10}	*p*-xylene	8.44	8.38	8.45
51	C_4H_3	CH_2CCCH	8.02[c]	8.08		107	C_7H_9N	benzylamine	8.73	8.77	
51	C_3HN	propiolonitrile	11.62	11.58	11.61	107	C_6H_5NO	2-pyridinecarboxaldehyde	9.75		9.69
52	C_4H_4	vinylacetylene	9.58	9.57	9.57	108	C_8H_{12}	1-vinyl-3-cyclohexene	8.93	8.94	
52	C_4H_4	1,2,3-butatriene	9.25	9.24		109	C_6H_7NO	1-methyl-4-pyridinone	8.48	8.51	
53	C_4H_5	CH_3CCCH_2	7.95[c]	7.93		109	C_6H_7NO	6-methyl-2-pyridinol	8.33		8.30
		CH_3CHCCH	7.97[c]			110	$C_5H_6N_2O$	1-oxide-3-pyridinamine	8.21	8.27	
53	C_3H_3N	2-propenenitrile	10.91	10.91	10.91	111	$C_5H_5NO_2$	4-pyridinol 1-oxide	8.18		8.30
54	C_4H_6	1,3-butadiene	9.07	9.05	9.10	116	C_9H_8	phenylallene	8.29	8.29	
54	C_3H_2O	2-propynol	10.7		10.70	117	C_8H_7N	indolizine	7.26	7.33	
55	C_3H_5N	2-propen-1-imine	9.65	9.70	9.65	117	C_8H_7N	benzylisonitrile	9.39	9.43	9.41
56	$C_2H_4N_2$	2,3-diazabutadiene	8.95	8.99	8.97	118	C_9H_{10}	*m*-vinyltoluene	8.37	8.40	
56	C_3H_4O	methylketene	8.95			118	C_9H_{10}	2-propenylbenzene	9.16		9.2
56	C_3H_4O	2-propenal	10.11		10.18	119	C_7H_5NO	benzonitrile oxide	8.96	8.93	8.98
58	C_3H_6O	propanal	9.96		9.98	120	C_8H_8O	acetophenone	9.28	9.18	9.24
64	C_5H_4	1,3-pentadiyne	9.4	9.33		127	$C_7H_{13}NO$	cycloheptanone oxime	8.88	8.85	
65	C_5H_5	cyclopentadienyl radical	8.41	8.49		128	$C_8H_4N_2$	isocyanobenzonitrile	9.28[d]	9.48	
65	C_4H_3N	cyanoallene	10.35	10.43	10.40	129	C_9H_7N	quinoline	8.63	8.63	
66	C_5H_6	1,2,4-pentatriene	8.88		8.82	130	$C_8H_6N_2$	1,8-naphthyridine	9.2	9.35	
66	C_5H_6	1,3-cyclopentadiene	8.57	8.57		131	C_9H_9N	*N*-methylindole	7.74	7.76	
67	C_4H_5N	pyrrole	8.21	8.21	8.21	132	$C_{10}H_{12}$	*o*-allyltoluene	7.78	7.93	
67	C_4H_5N	2-butenenitrile	10.23	10.18	10.18	142	$C_{11}H_{10}$	2-methylnaphthalene	7.91	7.82	
74	C_6H_2	1,3,5-hexatriyne	9.50	9.48		144	$C_{10}H_8O$	1-naphthalenol	7.76		7.82
75	C_3H_9NO	methoxyethylamine	9.45	9.45		144	$C_{11}H_{12}$	1,2,3,4-tetrahydro-1-methylene−naphthalene	7.90	7.73	
75	$C_2H_5NO_2$	nitrous ethyl ether	10.53	10.57		144	$C_{11}H_{12}$	2-cyclopenten-1-ylbenzene	9.2	9.33	
76	C_6H_4	hexa-1,5-diyne-3-ene	9.10	9.12		154	$C_{12}H_{10}$	biphenyl	8.9	9.13	
77	C_5H_3N	cyanovinylacetylene	9.33[d]	9.33		156	$C_{10}H_8N_2$	2,2′-bipyridine	8.6	8.64	8.64
78	C_6H_6	benzene	9.24	9.24	9.23						

[a] Refers to ref 21 except for specific description. [b] Errors for stable species are ±0.05 eV, for radicals they are ±0.10 eV. [c] Refers to ref 38. [d] Refers to ref 39.

mass peaks ranging from *m/e* 15 to 156 are observed, which correspond to hydrocarbon, oxygenated, and nitrogenous species. They could be combustion intermediates or fragment ions from photoionization. It is obvious that the number, position, and relative intensity of peaks are different between the rich and lean pyridine flames, especially for molecular weights heavier than pyridine. Isomers or different molecules with the same weight that could play different roles in the oxidation mechanism increase rapidly with increasing molecular weight. Thus, the isomeric identification of flame species is desired. In this study, most observed combustion intermediates are identified, which are listed in Table 1 along with literature IEs.[21] We will discuss nitrogenous, oxygenated, and hydrocarbon intermediates in the pyridine flames below.

3.1. Identification of Nitrogenous Intermediates. According to Alzueta et al.′s study, NO is formed through complex pathways involving a large number of nitrogenous intermediates, i.e., amino, cyanide, and other species.[14] Therefore, identification of nitrogenous intermediates is very useful for understanding the transformation of nitrogen atom. The most common nitrogenous intermediates are amines (ammonia, methanimine, 2-propen-1-imine, aniline, etc.) and nitriles (methyl isonitrile, propiolonitrile, 2-propenenitrile, 2-butenenitrile, etc.). These species were also identified in combustion studies of other

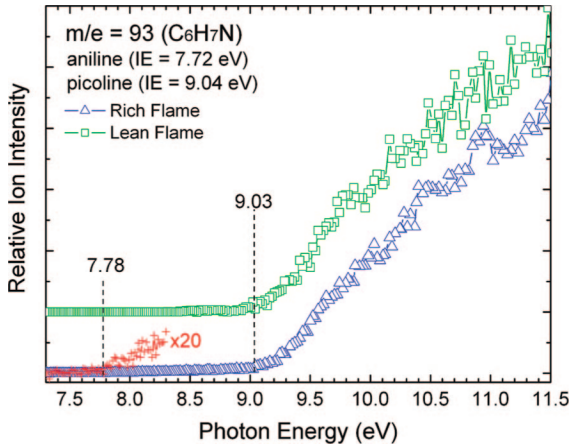

Figure 2. Stack plot of PIE spectra of *m/e* 93 (C_6H_7N) measured in the fuel-lean and -rich pyridine/O_2/Ar flames. The accepted ionization energies for proposed species are indicated in the figure.

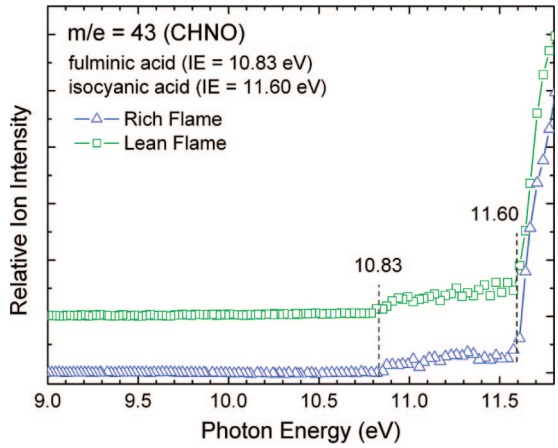

Figure 3. Stack plot of PIE spectra of *m/e* 43 (CHNO) measured in the fuel-lean and -rich pyridine/O_2/Ar flames. The accepted ionization energies for proposed species are indicated in the figure.

heterocyclic nitrogenous compounds.[22] Besides amines and nitriles, there are a number of other nitrogenous intermediates detected in the pyridine flames in this work, including C_4H_3N, C_4H_5N, C_5H_3N, C_5H_7N, C_6H_5N, C_6H_7N, $C_6H_{11}N$, C_7H_5N, C_7H_7N, C_7H_9N, C_8H_7N, C_9H_7N, C_9H_9N, HCNO, HNCO, CH_3NO, C_3H_9NO, C_5H_5NO, C_6H_5NO, C_6H_7NO, C_7H_5NO, $C_7H_{13}NO$, $C_2H_5NO_2$, $C_5H_5NO_2$, $C_5H_6N_2O$, $C_6H_4N_2$, $C_8H_4N_2$, $C_8H_6N_2$, $C_{10}H_8N_2$, etc. Most of these species have not been reported in previous investigations of pyridine oxidation.

PIE spectra, shown in Figures 2 and 3, illustrate isomeric identification of nitrogenous intermediates. Figure 2 displays the PIE spectrum of *m/e* 93. Two onsets at 7.78 and 9.02 eV are clearly observed from the PIE spectra in the rich flame, which are in accordance with IEs of aniline (IE = 7.72 eV[21]) and picoline (IE = 9.02−9.04 eV[21]). Thus, mass 93 includes the contributions of aniline and picoline in the rich flame, both of which are nitrogenous intermediates. However, only one onset on the PIE spectrum is observed for the lean flame, which could include contributions of picoline and/or phenoxy radical (C_6H_5O), since both species have close IEs.

The PIE spectrum of *m/e* 43 is shown in Figure 3. Two isomers, fulminic acid (HCNO, IE = 10.83 eV[21]) and isocyanic acid (HNCO, IE = 11.60 eV[21]), are formed in both the rich and lean flames. HNCO is a key nitrogenous intermediate in the oxidation of nitrogenous compounds since it can be utilized to reduce the amount of NO_x, which is in agreement with the conclusion of the previous investigations.[22] HNCO is mainly formed from the reaction of HCN and O/OH, and then converted to NH and CO.[23] HCNO was reported to be the major product of the CH_2 + NO reaction.[23] In this study, it can also be produced from decomposition of some nitrogenous intermediates such as pyridine oxide. Furthermore, the reaction of HC′C−CH=CH−CN with O atom is another formation source. According to the ab initio quantum chemical study and QRRK calculations, HNCO and HCNO can convert to each other and the former is more stable.[23] Isomerization of HCNO to HNCO is a major consumption channel of HCNO.[23] In addition, recombination of HCNO and other radicals, followed by dissociation including HCNO + O → HC(O)NO → HCO + NO and HCNO + OH → HC(OH)NO → HCHO + NO, is also dominant for HCNO consumption under flame conditions.[23] HCO is not observed in this work, because it is very reactive and could be quenched on the nozzle surface.

Some nitriles are formed in the pyridine flames as well, which is similar to the pyrrole flames.[22] For instance, propiolonitrile (C_3HN) and 2-propenenitrile (C_3H_3N) are identified in both rich and lean pyridine flames. C_3HN was detected as a major nitrogenous product in the shock tube study of pyridine.[8] Decomposition of C_3H_3N/C_5H_4N and reaction of C_2H with HCN may account for its formation.[8] Besides C_3HN, a hydrocarbon radical C_4H_3 is identified in the rich flame. It can be formed from the decomposition of *m*-C_5H_4N/*p*-C_5H_4N according to the reaction mechanism of pyridine pyrolysis proposed by Kiefer et al.[9] Its possible consumption channels are H/CN/CHCHCN addition reactions and sequential conversion to C_2H_2 and/or C_4H_2.[9] 2-Propenenitrile could be formed from the combination of C_2H_2 and HCN[8] or through reactions of CHCHCN and H/C_5H_5N.[9] Two C_4H_5 isomers, CH_3CCCH_2 and CH_3CHCCH, can also contribute to mass 53 in the rich pyridine flame. However, the C_4H_5 radical is not observed in the lean flame, which could be due to its low concentration.

Similarly, mass 103 includes benzoisonitrile (C_7H_5N) in both flames. It should be noted that benzonitrile, an isomer of benzoisonitrile, is only identified in the rich flame. This may result from the difference of the stability of the two isomers, and benzonitrile could be easily consumed in the lean flame. Moreover, the addition of acetonitrile to cyclopentadienyl radical may lead to the production of benzonitrile, while cyclopentadienyl is not formed in the lean flame. Benzonitrile had been measured in a single-pulse shock tube by Mackie et al. using capillary column GC together with GC/MS and FTIR spectroscopy. However, they did not observe benzoisonitrile.[8]

The heaviest intermediate identified in the pyridine flames is 2,2′-bipyridine ($C_{10}H_8N_2$). The self-combination of *o*-pyridyl is considered to be its major formation channel. We have not detected *o*-pyridyl in this work. Since it is very reactive and unstable, it may be quenched on the nozzle surface. As listed in Table 1, other nitrogenous intermediates are also identified, along with the literature values as well. It should be noted that HCN/HNC and CH_3CN are not measured in this study because of the cutoff limitation of the LiF window. These species are believed to be abundant in the pyridine flames, which will be studied with a newly constructed beamline from undulator radiation in the future.

3.2. Identification of Oxygenated Intermediates. A number of oxygenated intermediates are identified in the pyridine flames as well. Figure 4 shows PIE spectra of *m/e* 44 in the two flames. Two onsets close to 9.33 and 10.23 eV on the PIE spectra correspond to ionizations of two C_2H_4O isomers, ethenol and acetaldehyde, both of which have been identified in the pyrrole flames also.[22] To estimate the composition of two isomers, the

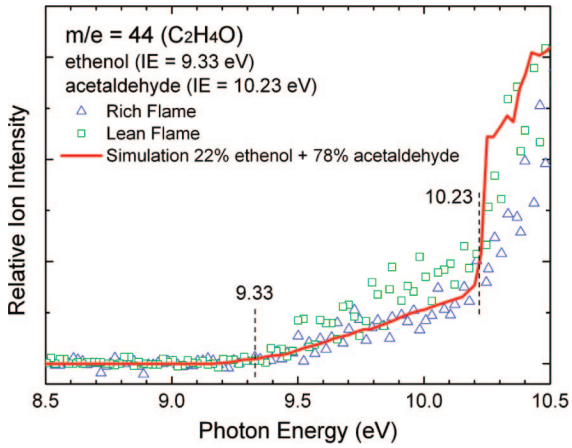

Figure 4. Scaled PIE spectra of *m/e* 44 (C_2H_4O) measured in the fuel-lean and -rich pyridine/O_2/Ar flames. The accepted ionization energies for ethanol and acetaldehyde are indicated in the figure. The solid line shows the computed average photoionization cross section for a mixture of 22(±5)% ethenol and 78(±5)% acetaldehyde.

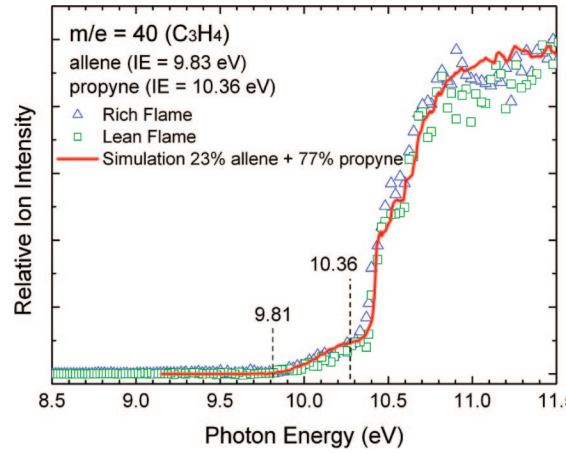

Figure 5. Scaled PIE spectra of *m/e* 40 (C_3H_4) measured in the fuel-lean and -rich pyridine/O_2/Ar flames. The accepted ionization energies for allene and propyne identified by the observed ionization thresholds are indicated in the figure. The solid line shows the computed average photoionization cross section for a mixture of 23(±5)% allene and 77(±5)% propyne.

ion signals are scaled to match a solid line showing the photoionization cross section[24] calculated for a best-fit isomeric composition of 22(±5)% ethenol and 78(±5)% acetaldehyde for the two flames. Ethenol is identified as a common intermediate in various hydrocarbon flames[15,25] and some oxygenated fuel flames.[26] However, it had not been detected in flames of nitrogenous fuels except in the pyrrole flames studied recently. It is suggested that the reaction of ethylene and OH is the dominant source of ethenol in hydrocarbon flames,[25,27] which may be applied to nitrogenous compounds flames. Moreover, addition and elimination reactions of OH with other alkenes are also likely to be responsible for ethenol formation in the pyridine flames. For acetaldehyde, it can be produced from the decomposition of 2-pyridinol and/or isomerization of ethenol.

Ketene is identified in both rich and lean flames, which is also observed in the pyrrole flames.[22] It can be formed through the oxidation of acetylene[28] and/or decomposition of C_5H_5NO and consumed in the C_1-oxidation pathway. Besides C_2H_2O and C_2H_4O, other oxygenated intermediates, such as formaldehyde (HCHO), formic acid (CH_2O_2), 2-propynol (C_3H_2O), methylketene/2-propenal (C_3H_4O), propanol (C_3H_6O), phenol (C_6H_6O), acetophenone (C_8H_8O), and 1-naphthalenol ($C_{10}H_8O$) are also identified in the pyridine flames, which are also listed in Table 1. PIE spectra measurement shows that formic acid (CH_2O_2) is formed only in the lean flame. It could be produced through the oxidation of formaldehyde. However, CH_2O_2 is not observed in the rich flame, which is reasonable since oxygenated intermediates are difficult to form under fuel-rich conditions, especially for those containing more than one oxygen atom. According to measurement of PIE spectra of *m/e* 56, the onset observed at 8.97 eV in the two flames suggests the existence of 2,3-diazabutadiene ($C_2H_4N_2$) and/or methylketene (*m*-C_3H_4O) because they have the same IEs of 8.95 eV.[21] We suggest that *m*-C_3H_4O as the dominant species in the lean flame since it can be formed more easily and more stable than $C_2H_4N_2$ under fuel-lean conditions. On the other hand, $C_2H_4N_2$ can be formed via self-combination and sequentially hydrogen elimination reaction of methanimine, which is also observed in this study. Another onset at 10.18 eV observed in the PIE spectra of mass 56 in the lean flame corresponds to 2-propenal (2-C_3H_4O, IE = 10.11 eV[21]). According to previous study, the two isomers *m*-C_3H_4O and 2-C_3H_4O can convert to each other.[29]

Mass 94 is identified to be phenol (C_6H_6O) formed in the both flames, which can be produced from the reactions of H + phenoxy and/or OH + C_6H_5. Among the oxygenated combustion intermediates mentioned above, HCHO, C_2H_4O, C_3H_2O, C_3H_4O, C_3H_6O, C_6H_6O, C_8H_8O, and $C_{10}H_8O$ have not been observed in thermal decomposition/oxidation of pyridine previously. These species should be involved in a more complete kinetic model for pyridine flames.

3.3. Identification of Hydrocarbon Intermediates. Although the oxidation of pyridine is a complicated chemical process that contains many nitrogenous and oxygenated intermediates as discussed above, the function of hydrocarbon intermediates cannot be ignored in the oxidation process of pyridine. Hydrocarbons play significant roles in reaction mechanisms and contribute to the formation of benzene, PAHs, and soot under flame conditions. In the present work, more than 35 hydrocarbons, including radicals and stable intermediates with carbon number from C_1 to C_{12}, are detected and identified, which are listed in Table 1 as well.

The smallest hydrocarbon species detected in the two flames is methyl radical, which can be formed through the reaction of acetylene and hydroxyl radical.[28] CH_3 can react with H_2, C_2H, and C_5H_5N to form CH_4, C_3H_4, and C_5H_4N.[8] Propargyl radical (C_3H_3), a key radical in forming aromatic or PAH compound[30−33] and a common intermediate in hydrocarbon and pyrrole flames, is also identified in the pyridine flames. It was considered in the reaction model of the pyridine pyrolysis.[8] Besides these two radicals, C_3H_5, C_3H_7, C_4H_3, C_4H_5, C_5H_5, and C_8H_9 are also detected in the pyridine flames.

C_2H_2 was measured as one of the major products in pyrolysis of pyridine,[3−5,8] which is also detected in this study. It can be the decomposition product of *o*-pyridyl[9] and/or C_5H_5NO.[14] According to Martoprawiro et al.'s study, acetylene and ethylene can convert to each other.[34] C_2H_2 could be a major precursor of C_6H_5 radical by reacting with C_4H_3 radical.[8] Moreover, It can be easily consumed by O/OH in the preflame zone.[28]

Figure 5 presents PIE spectra of mass 40 sampled from the lean and rich flames. The scaled PIE spectra in both flames are almost identical, indicating the same composition between the two flames. Two onsets at 9.81 and 10.36 eV are observed clearly, which can be ascribed to ionizations of two isomers, allene (*a*-C_3H_4, IE = 9.83 eV[21]) and propyne (*p*-C_3H_4, IE = 10.36 eV[21]), respectively. To estimate the composition of mass 40, the ion signals are scaled to match a solid line showing the

photoionization cross section[24] calculated for a best-fit isomeric composition of 23(±5)% allene and 77(±5)% propyne for the two flames. Although C_3H_4 was reported as the pyrolysis product by Mackie et al., the isomers had not been distinguished in their previous studies.[8]

Vinylacetylene (v-C_4H_4) is identified in both the lean and rich flames. However, 1,2,3-butatriene (b-C_4H_4) is detected only in the rich flame. v-C_4H_4 is thought to be the self-combination product of C_2H_2 and could dissociate to C_4H_2 and H_2.[35] In addition, C_4H_4 can convert to C_4H_5 and C_4H_6. C_4H_5 is only observed in the rich flame.

Mass 66 is identified to be 1,2,4-pentatriene (p-C_5H_6) for the lean flame and is confirmed to be 1,3-cyclopentadiene (c-C_5H_6) for the rich flame. c-C_5H_6 can lose an H atom to form cyclopentadienyl radical, which is also identified in the rich flame and could convert to benzene through further conversion. Toluene (C_7H_8), the simplest monosubstituted aromatic molecule, is also detected in the two flames. The primary species observed in pyrolysis studies of toluene were C_2H_2, C_4H_2, and CH_4.[36,37] Two pathways, $C_5H_5 + C_2H_2 \rightarrow C_6H_5CH_2 \rightarrow C_7H_8$ and $C_4H_4 + H_2CCCH \rightarrow C_6H_5CH_2 \rightarrow C_7H_8$, were considered for its formation.[37] The hydrocarbon intermediates mentioned above, except for C_2H_2, C_2H_4, C_3H_4, C_4H_2, C_4H_4, C_6H_2, and C_6H_6, have not been observed in previous thermal decomposition/oxidation studies of pyridine.

On the basis of the experimental measurement in this work, the formation of tricyclic or larger species is neglectable for the ring growth process, which may result from two reasons. On one hand, the N atom in the heterocycle will reduce the aromaticity and inhibit the addition of C_2H_2 or C_4H_2 and subsequent ring closure, which is in accordance with previous studies. On the other hand, the formation of larger species could be restricted by low-concentration hydrocarbon radicals like C_3H_3, C_4H_3, and C_5H_5 which are responsible for aromatics formation.

4. Conclusion

Two low-pressure premixed pyridine/oxygen/argon flames with equivalence ratios of 0.56 and 2.10 have been investigated with tunable synchrotron VUV photoionization and molecular-beam mass spectrometry techniques. Most nitrogenous, oxygenated, and hydrocarbon combustion intermediates with mass ranging from 15 to 156 in the two flames have been identified according to the measurements of photoionization mass spectra and photoionization efficiency spectra. Many new species, especially nitrogenous ones such as methanimine, methyl isonitrile, fulminic acid, isocyanic acid, 2-propen-1-imine, 2,3-diazabutadiene, cyanoallene, 2-butenenitrile, 2-methylpyrrole, phenylnitrene, picoline, pyridine oxide, 2-pyridinol, etc. are detected in this work. The results indicate that the N conversion is mainly initiated through (1) H abstraction and O addition reactions to form pyridine oxide, 2-pyridinol, and o-pyridyl radical, which then undergo a subsequent series of reactions to form the final products, and (2) reactions with unsaturated small hydrocarbon intermediates to form bicyclic species including indolizine (C_8H_7N), quinoline (C_9H_7N), and 1,8-naphthyridine ($C_8H_6N_2$) etc.

By comparison of the intermediates pool, it is found that CH_2CCCH, 1,2,3-butatriene, CH_3CCCH_2/CH_3CHCCH, 1,3-pentadiyne, cyclopentadienyl radical, 1,3-cyclopentadiene, 1,3,5-hexatriyne, cyanovinylacetylene, aniline, phenylacetylene, benzonitrile, 4-methylbenzyl radical, *N*-phenylmethanimine, benzylamine, 1-methyl-4-pyridinone, phenylallene, indolizine, m-vinyltoluene, cycloheptanone oxime, isocyanobenzonitrile, quinoline, 1,8-naphthyridine, *N*-methylindole, o-allyltoluene, 2-methylnaphthalene, biphenyl, etc. are observed only in the rich flame, while methanol, formamide, formic acid, 2-propynol, 2-propenal, propanal, 1,2,4-pentatriene, diallylamine, 2-vinylpyridine, 2-pyridinecarboxaldehyde, 6-methyl-2-pyridinol, 4-pyridinol 1-oxide, 2-propenylbenzene, and 1-naphthalenol exist only in the lean flame. Furthermore, the experiment proves that it is difficult to form PAHs with tricyclic or larger species in the pyridine flames. The experimental observations are useful for further insight into the combustion chemistry of nitrogenous fuels.

Acknowledgment. F.Q. is grateful for the funding support from the Chinese Academy of Sciences, the Specialized Research Fund for the Doctoral Program of Higher Education, Natural Science Foundation of China under Grant no. 20533040, National Basic Research Program of China (973) under Grant no. 2007CB815204, and Ministry of Science and Technology of China under Grant no. 2007DFA61310.

References and Notes

(1) Miller, J. A.; Bowman, C. T. *Prog. Energy Combust. Sci.* **1989**, *15*, 287.
(2) Roth, C. F. *Chem. Ber.* **1886**, *19*, 360.
(3) Hurd, C. D.; Simon, J. I. *J. Am. Chem. Soc.* **1962**, *84*, 4519.
(4) Axworthy, A. E.; Dayan, V. H.; Martin, G. B. *Fuel* **1978**, *57*, 29.
(5) Houser, T. J.; McCarville, M. E.; Biftu, T. *Int. J. Chem. Kinet.* **1980**, *12*, 555.
(6) Kern, R. D.; Yong, J. N.; Kiefer, J. H.; Shah, J. N. *Int. Symp. Shock Tubes Waves, 16th* **1987**, *16*, 437.
(7) Leidreiter, H. I.; Wagner, H. G. *Z. Phys. Chem. N. F.* **1987**, *153*, 99.
(8) Mackie, J. C.; Colket, M. B.; Nelson, P. F. *J. Phys. Chem.* **1990**, *94*, 4099.
(9) Kiefer, J. H.; Zhang, Q.; Kern, R. D.; Yao, J.; Jursic, B. *J. Phys. Chem. A* **1997**, *101*, 7061.
(10) Hore, N. R.; Russell, D. K. *J. Chem. Soc., Perkin Trans.* **1998**, *2*, 269.
(11) Memon, H. U. R.; Bartle, K. D.; Taylor, J. M.; Williams, A. *Int. J. Energy Res.* **2000**, *24*, 1141.
(12) Houser, T. J.; McCarville, M. E.; Houser, B. D. *Combust. Sci. Technol.* **1982**, *27*, 183.
(13) Ikeda, E.; Nicholls, P.; Mackie, J. C. *Proc. Combust. Inst.* **2000**, *28*, 1709.
(14) Alzueta, M. U.; Tena, A.; Bilbao, R. *Combust. Sci. Technol.* **2002**, *174*, 151.
(15) Cool, T. A.; Nakajima, K.; Mostefaoui, T. A.; Qi, F.; McIlroy, A.; Westmoreland, P. R.; Law, M. E.; Poisson, L.; Peterka, D. S.; Ahmed, M. *J. Chem. Phys.* **2003**, *119*, 8356.
(16) Qi, F.; Yang, R.; Yang, B.; Huang, C. Q.; Wei, L. X.; Wang, J.; Sheng, L. S.; Zhang, Y. W. *Rev. Sci. Instrum.* **2006**, *77*, 084101.
(17) Cool, T. A.; Nakajima, K.; Taatjes, C. A.; McIlroy, A.; Westmoreland, P. R.; Law, M. E.; Morel, A. *Proc. Combust. Inst.* **2005**, *30*, 1681.
(18) Yang, B.; Li, Y. Y.; Wei, L. X.; Huang, C. Q.; Wang, J.; Tian, Z. Y.; Sheng, L. S.; Zhang, Y. W.; Qi, F. *Proc. Combust. Inst.* **2007**, *31*, 555.
(19) Yang, B.; Osswald, P.; Li, Y. Y.; Wang, J.; Wei, L. X.; Tian, Z. Y.; Qi, F.; K.-Höinghaus, K. *Combust. Flame* **2007**, *148*, 198.
(20) Huang, C. Q.; Yang, B.; Yang, R.; Wang, J.; Wei, L. X.; Shan, X. B.; Sheng, L. S.; Zhang, Y. W.; Qi, F. *Rev. Sci. Instrum.* **2005**, *76*, 126108.
(21) Linstrom, P. J.; Mallard, W. G., Eds. *NIST Chemistry Webbook, NIST Standard Reference*; Database No. 69, June 2005, National Institute of Standards and Technology, Gaithersburg, MD (http://webbook.nist.gov/chemistry).
(22) Tian, Z. Y.; Li, Y. Y.; Zhang, T. C.; Zhu, A. G.; Cui, Z. F.; Qi, F. *Combust. Flame* **2007**, *151*, 347.
(23) Gardiner, W. C. *Gas-Phase Combustion Chemistry*; Springer-Verlag: New York, 1999; p 197.
(24) Cool, T. A.; McIlroy, A.; Qi, F.; Westmoreland, P. R.; Poisson, L.; Peterka, D. S.; Ahmed, M. *Rev. Sci. Instrum.* **2005**, *76*, 094102.
(25) Taatjes, C. A.; Hansen, N.; McIlroy, A.; Miller, J. A.; Senosiain, J. P.; Klippenstein, S. J.; Qi, F.; Sheng, L. S.; Zhang, Y. W.; Cool, T. A.; Wang, J.; Westmoreland, P. R.; Law, M. E.; Kasper, T.; K.-Höinghaus, K. *Science* **2005**, *308*, 1887.
(26) Li, Y. Y.; Wei, L. X.; Tian, Z. Y.; Yang, B.; Wang, J.; Zhang, T. C.; Qi, F. *Combust. Flame* **2008**, *152*, 336.

(27) Taatjes, C. A.; Hansen, N.; Miller, J. A.; Cool, T. A.; Wang, J.; Westmoreland, P. R.; Law, M. E.; Kasper, T.; K.-Höinghaus, K. *J. Phys. Chem. A* **2006**, *110*, 3254.

(28) Ancia, R.; Tiggelen, P. J. V.; Vandooren, J. *Exp. Therm. Fluid Sci.* **2004**, *28*, 715.

(29) Turecek, F.; Drinkwater, D. E.; Mclafferty, F. W. *J. Am. Chem. Soc.* **1991**, *113*, 5958.

(30) Frenklach, M.; Clary, D. W.; Gardiner, W. C.; Stein, S. E. *Proc. Combust. Inst.* **1984**, *20*, 887.

(31) Marinov, N. M.; Castaldi, M. J.; Melius, C. F.; Tsang, W. *Combust. Sci. Technol.* **1997**, *128*, 295.

(32) Miller, J. A.; Klippenstein, S. J. *J. Phys. Chem. A* **2003**, *107*, 7783.

(33) McEnally, C. S.; Pfefferle, L. D.; Atakan, B.; Kohse-Höinghaus, K. *Prog. Energy Combust. Sci.* **2006**, *32*, 247.

(34) Martoprawiro, M.; Bacskay, G. B.; Mackie, J. C. *J. Phys. Chem. A* **1999**, *103*, 3923.

(35) Mackie, J. C.; Colket, M. B.; Nelson, P. F.; Esler, M. *Int. J. Chem. Kinet* **1991**, *23*, 733.

(36) Pamidimukkala, K. M.; Kern, R. D.; Patel, M. R.; Wei, H. C.; Kiefer, J. H. *J. Phys. Chem.* **1987**, *91*, 2148.

(37) Sivaramakrishnan, R.; Tranter, R. S.; Brezinsky, K. *J. Phys. Chem. A* **2006**, *110*, 9400.

(38) Hansen, N.; Klippenstein, S. J.; Taatjes, C. A.; Miller, J. A.; Wang, J.; Cool, T. A.; Yang, B.; Yang, R.; Wei, L. X.; Huang, C. Q.; Wang, J.; Qi, F.; Law, M. E.; Westmoreland, P. R. *J. Phys. Chem. A* **2006**, *110*, 3670.

(39) Note: A B3LYP method with the 6-31G(d) basis set is used for structure optimization and energy calculations of HCCCHCHCN(C_5H_3N), pyridyl radical (C_5H_4N), benzoisonitrile (C_7H_5N), and isocyanobenzonitrile ($C_8H_4N_2$).

JP8066537